

# Parameter identification in nonlinear models using periodic equilibrium states

**Citation for published version (APA):**

Kraker, de, A., Verbeek, G., & Wouw, van de, N. (1997). Parameter identification in nonlinear models using periodic equilibrium states. In D. H. Campen, van (Ed.), *Interaction between dynamics and control in advanced mechanical systems : proceedings of the IUTAM symposium, 21-26 April, 1996, Eindhoven, the Netherlands* (pp. 191-198). (Solid mechanics and its applications. SMIA; Vol. 52). Kluwer Academic Publishers.

**Document status and date:**

Published: 01/01/1997

**Document Version:**

Publisher's PDF, also known as Version of Record (includes final page, issue and volume numbers)

**Please check the document version of this publication:**

- A submitted manuscript is the version of the article upon submission and before peer-review. There can be important differences between the submitted version and the official published version of record. People interested in the research are advised to contact the author for the final version of the publication, or visit the DOI to the publisher's website.
- The final author version and the galley proof are versions of the publication after peer review.
- The final published version features the final layout of the paper including the volume, issue and page numbers.

[Link to publication](#)

**General rights**

Copyright and moral rights for the publications made accessible in the public portal are retained by the authors and/or other copyright owners and it is a condition of accessing publications that users recognise and abide by the legal requirements associated with these rights.

- Users may download and print one copy of any publication from the public portal for the purpose of private study or research.
- You may not further distribute the material or use it for any profit-making activity or commercial gain
- You may freely distribute the URL identifying the publication in the public portal.

If the publication is distributed under the terms of Article 25fa of the Dutch Copyright Act, indicated by the "Taverne" license above, please follow below link for the End User Agreement:

[www.tue.nl/taverne](http://www.tue.nl/taverne)

**Take down policy**

If you believe that this document breaches copyright please contact us at:

[openaccess@tue.nl](mailto:openaccess@tue.nl)

providing details and we will investigate your claim.

# PARAMETER-IDENTIFICATION IN NONLINEAR MODELS USING PERIODIC EQUILIBRIUM STATES

A. DE KRAKER, G. VERBEEK AND N. VAN DE WOUW  
*Department of Mechanical Engineering,  
Eindhoven University of Technology,  
P.O. Box 513, 5600 MB Eindhoven, The Netherlands*

## 1. Introduction

For the identification of parameters in numerical models for nonlinear dynamical systems often transient trajectories (for example resulting from drop-tests for aircraft landing gears) or chaotic trajectories are used as input information for the identification procedure. Instead of these types of trajectories the use of stable or even unstable periodic solutions has some clear advantages such as the possibility of use for a future design optimization for a landing gear or the possibility of a huge data-reduction in the case of a chaotic signal. In the following, first a method for calculating **stable** as well as **unstable** periodic solutions and a Bayesian estimation procedure will be presented. Next two applications of parameter identification will be given, referring to a landing gear with stable, non-smooth periodic solutions and to a pendulum exhibiting a chaotic trajectory, in which case multiple, smooth unstable periodic solutions will be applied.

## 2. Periodic Equilibrium States

We consider the ordinary differential equations  $g$  of a structural system in the degrees of freedom  $q$ , and corresponding output equations  $\hat{y}$ :

$$g(q, q', q'', F, \tau, \theta) = 0, \quad \hat{y} = f(q, q', q'', F, \tau, \theta). \quad (1)$$

The  $l$ -dimensional vector  $\theta$  stands for the uncertain model parameters. The external forcing frequency is  $f_e$  (period  $T_e = 1/f_e$ ),  $F$  stands for the periodic excitation force. A nondimensional time variable  $\tau$ ,  $\tau \in [0, 1]$  is introduced as  $\tau = f_e t$ , where the prime ( $'$ ) stands for differentiation with respect to  $\tau$ . For details see [1] and [4]. An approximate periodic response can be ob-

tained by application of an equidistant discretization procedure. The time variable  $\tau$  is discretized using  $n$  time intervals:  $\tau_\mu = (\mu - 1)\Delta\tau$ ,  $\mu \in \{1, 2, \dots, n\}$ ,  $\Delta\tau = 1/n$ . All time dependent variables are also discretized and will be subscripted by  $\mu$  on time step  $\tau_\mu$ . The discretized degrees of freedom  $q_\mu$  are stored in the column  $z = [q_1^T, q_2^T, \dots, q_n^T]^T$ .

Subsequently, the derivatives of the discretized degrees of freedom  $q_\mu$  can be approximated by any difference scheme. For the landing gear identification a second order backward scheme for both the first and second derivatives appeared to perform best (i.e. showed no occurrence of numerical instabilities due to the non-smooth character of the response, for sufficiently fine time grids with  $n \approx 800$ ). For the pendulum problem a  $2^{nd}$  order central difference scheme was successfully applied. For periodic solutions we have the additional boundary condition:

$$q_i = q_{i \pm n}, \quad i \notin \{1, 2, \dots, n\} \quad \wedge \quad i \pm n \in \{1, 2, \dots, n\}. \quad (2)$$

Now for each time step  $\tau_\mu$  a set of approximate difference and discrete output equations can be derived  $\tilde{g}_\mu(z, x_\mu, \tau_\mu, \theta) = 0$ ,  $\hat{y}_\mu = \tilde{f}_\mu(z, x_\mu, \tau_\mu, \theta)$  leading for all time steps to a set of nonlinear algebraic equations

$$\tilde{g}(z, x, \tau, \theta) \equiv [\tilde{g}_1^T, \tilde{g}_2^T, \dots, \tilde{g}_n^T]^T = 0, \quad (3)$$

which is solved for the discrete periodic solution  $z$  from an initial static equilibrium guess by a modified Newton procedure, making use of the decomposition technique and a robust step halving technique as proposed in [1]. Substitution of  $z$  in the discretized output equations will give the requested output values  $\hat{y}_{\mu\kappa}$ .

For the Bayesian estimator used in this paper, the first derivatives of the outputs  $\hat{y}_{\mu\kappa}$  to the model parameters  $\theta$  are required and can be derived from

$$d\hat{y}_{\mu\kappa}/d\theta = \tilde{f}_{\mu\kappa,\theta} + [d\tilde{f}_{\mu\kappa}/dz]z_{,\theta}, \quad d\tilde{g}/d\theta = \tilde{g}_{,\theta} + [d\tilde{g}/dz]z_{,\theta} = 0. \quad (4)$$

The derivatives  $\tilde{f}_{\mu\kappa,\theta}$  and  $d\tilde{f}_{\mu\kappa}/dz$ , can be derived by hand or by symbolic computation. The remaining unknown partial derivatives  $z_{,\theta}$  follow from the so-called sensitivity equation  $d\tilde{g}/d\theta$ . The partial derivatives  $\tilde{g}_{,\theta}$  should also be derived by hand or by symbolic computations from the differential equations. The derivatives  $d\tilde{g}/dz$  follow directly from the last Newton iteration of the periodic solver.

### 3. Bayesian Estimation

We use a Bayesian estimator, see [4], for estimating the model parameters as well as unknown distribution parameters of the residuals, i.e. the difference between measured outputs  $y$  and predicted outputs  $\hat{y}$

$$e_{\mu\kappa}(\theta) \equiv y_{\mu\kappa} - f_{\mu\kappa}(q, \dot{q}, \ddot{q}, F(f_e), t, \theta) = y_{\mu\kappa} - \hat{y}_{\mu\kappa}. \quad (5)$$

We assume normally distributed  $\mathcal{N}_s(0, \text{diag}(v))$  residuals and also normally distributed  $\mathcal{N}_l(\bar{\theta}, \text{diag}(\sigma^2))$  a priori knowledge of the model parameters. Measurement errors and modelling errors are not distinguished and the total errors are assumed to be statistically independent over the  $n$  samples  $\mu$ , the  $N$  experiments  $\kappa$ , and the  $s$  measurement channels  $\beta$ . Now the Bayesian estimation problem leads to a maximization problem

$$\Phi_B(\theta, v_1, \dots, v_s) = -\frac{1}{2} \left[ nN \ln \prod_{\beta=1}^s v_\beta + \sum_{\beta=1}^s \frac{M_{\beta\beta}(\theta)}{v_\beta} + \sum_{\alpha=1}^l \frac{(\theta_\alpha - \bar{\theta}_\alpha)^2}{\sigma_\alpha^2} \right] \quad (6)$$

with 
$$M_{\beta\beta}(\theta) = \sum_{\kappa=1}^N \sum_{\mu=1}^n e_{\mu\kappa\beta}^2(\theta),$$

in which  $M_{\beta\beta}(\theta)$  stands for the diagonal terms of the moment matrix of the residuals. The estimation problem is solved iteratively by Newton-Gauss approximation of the Taylor series of the object function (7) by staged optimization. Firstly, from (7) the unknown measurement channel variances can be solved with bias correction for each iteration

$$v_\beta = \frac{s}{nNs - l} \sum_{\kappa=1}^N \sum_{\mu=1}^n e_{\mu\kappa\beta}^2. \quad (7)$$

Secondly the model parameter updating formula reads

$$\Delta\theta_i = \left( -H_{\theta\theta}^{-1} q_\theta \right)_i = - \left[ \sum_{\kappa=1}^N \sum_{\mu=1}^n e_{\mu\kappa,\theta}^T \text{diag}(v)^{-1} e_{\mu\kappa,\theta} + \text{diag}(w)^{-1} \right]_i^{-1} \\ \times \left( \sum_{\kappa=1}^N \sum_{\mu=1}^n e_{\mu\kappa,\theta}^T \text{diag}(v)^{-1} e_{\mu\kappa} \right)_i \quad \text{with } w = (\sigma_1^2, \dots, \sigma_l^2)^T. \quad (8)$$

in which  $H_{\theta\theta}$  stands for the  $\theta$ -partition of the Hessian of the object function (7) and  $q_\theta$  is the corresponding partition of the gradient. The first order derivatives  $e_{\mu\kappa,\theta} = -\hat{y}_{\mu\kappa,\theta}$  can be computed efficiently from a large set of periodic algebraic sensitivity equations (4). For more information on the estimator, the solution procedure or the computation of derivative information the reader is referred to [4].

## 4. Landing Gear Identification

### 4.1. MODEL DESCRIPTION AND EXPERIMENTAL SET-UP

The identification procedure will first be illustrated for identifying parameters of a simplified F-16 nose landing gear damper under periodic excitation. With hydraulic equipment, a periodic axial displacement has been exerted on the landing gear, measuring the force acting on the wheel axle and the internal gas pressure of the damper. For more information see [4],[5]. The

basic model for this damper reads:

$$\begin{aligned} \theta_1(\ddot{q} + \theta_2) + \theta_3\dot{q}|\dot{q}| + \theta_4p + (\theta_8 + \theta_9p) \arctan(\theta_{10}\dot{q}) + \theta_{11} - F_e &= 0, \\ \theta_{15}\dot{T} + \theta_{16}(1 + \theta_6q)(T + \theta_{17}) - (\theta_4p + \theta_{11})\dot{q} &= 0, \\ \text{with } p = \theta_5T/(1 + \theta_6q + \theta_7T), \quad \hat{y} = q + \theta_{12}. \end{aligned} \quad (9)$$

The mechanical model (1st. equation) includes inertia, velocity squared oil damping, a nitrogen gas spring approximated by polytropic ideal gas behaviour and a continuous approximation of Coulomb friction, whereas the thermo-dynamical model (2nd. equation) includes a gas heat capacity, cylinder-wall heat conduction and a source term due to gas compression and extension. Some of the 15 parameters  $\theta_k$  can be determined rather accurately in advance, some of them could not be identified due to limited hydraulic power (especially the damping parameter  $\theta_3$ ) and some parameters haven't been extracted directly from the measurement data. The identification-procedure has been applied to estimate the 3 most important and uncertain parameters, namely  $\theta_4$ ,  $\theta_6$  and  $\theta_{16}$ . Due to limited hydraulic

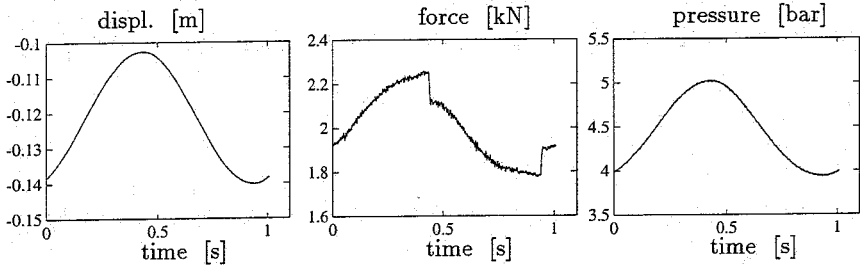


Figure 1. Frequency 1 Hz, small amplitude ( $\pm 18$  mm), experiment 920713m1.

power but also for reasons of efficiency a set of experiments was defined that covers the total available system state and parameter space. This resulted in a set of 14 large-stroke-low-frequency up to small-stroke-high-frequency experiments.

For the excitation a controlled sinusoidal axial displacement was selected. Typical time histories of the measurements are shown in Fig. 1. The figure shows the nearly perfect sinusoidal displacement signal, the force signal with significant force discontinuities at 0.5 and 1 s (friction), and smooth relative gas pressure signals.

#### 4.2. IDENTIFICATION RESULTS

In general the large amplitude residuals are less by half than the small amplitude residuals, also the spreads in parameters  $\theta_4$  and  $\theta_6$  are much smaller and acceptable. The heat conduction parameter  $\theta_{16}$  is not really constant, and for some small amplitude inputs the parameter is even negative which means that the heat transfer is still not modelled accurately

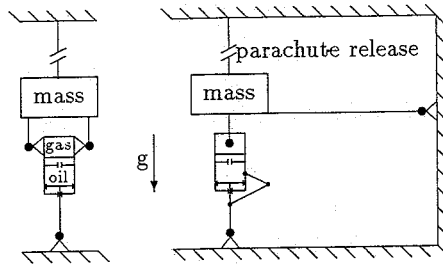


Figure 2. Schematic view of the laboratory drop-test set-up. Dimensions between the joints: landing gear height 1.16 m, width 0.58 m, pivoting frame length 2.02 m.

enough. For the verification of the feasibility of the shaker-test identification method a small number of (simplified) drop-test experiments have been performed, see Fig. 2 for a schematic view. The measurements start when a mass is suddenly set free, loading the damper. The experimental results and predicted outputs for a representative landing experiment are shown in Fig. 3. The measured quantities are plotted with solid lines and the predictions with dashed lines. The figures show that the amplitudes

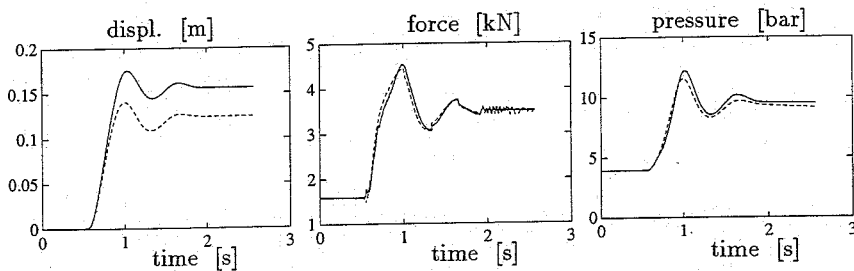


Figure 3. Predictions for drop-test experiment 930426c0

and the frequency of the oscillations in all three signals are predicted very well, but the displacement signal shows a large static offset component. However, at 2.5 s the gas temperature is not yet equal to the environmental temperature. Simulation for a longer time interval shows that the static equilibrium value is predicted correctly after approximately 30 s. Despite the good overall predictions for the force and pressure signals, it must be concluded that the thermo-mechanical model needs further research.

## 5. A Parametrically Excited Pendulum

### 5.1. MODEL DESCRIPTION

To illustrate the use of chaotic data in the estimation of structural parameters from a nonlinear mechanical system we investigated a parametrically excited pendulum as given in Fig. 4. In the top position the instantaneous angular position  $\phi$  and the angular velocity  $\dot{\phi}$  of the pendulum are measured, giving a point  $(\phi, \dot{\phi})$  in the Poincaré section; phase space points are

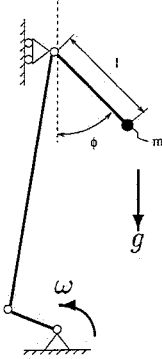


Figure 4. The parametrically driven pendulum

thus obtained with time intervals of  $\frac{2\pi}{\omega}$  s. The mathematical model reads:

$$\ddot{\phi} + \frac{k_1}{ml^2} \text{sgn}(\dot{\phi}) + \frac{k_2}{ml^2} \dot{\phi} + \frac{k_3}{ml^2} (\dot{\phi})^2 \text{sgn}(\dot{\phi}) + f_{exc}(\omega) \sin(\phi) = 0 \quad (10)$$

This equation includes inertia, Coulomb friction, viscous damping, air resistance and a driving force. At  $\omega = 13 \frac{\text{rad}}{\text{s}}$  the pendulum is in a rotating motion whose frequency is locked to the excitation. When decreasing  $\omega$ , we encounter a series of period-doubling bifurcations that finally lead to a large chaotic attractor at  $\omega = 9.09 \frac{\text{rad}}{\text{s}}$ , extending over the full angular range and shown in Fig. 5. For more details of the experimental set-up and nominal parameter values see [3].

## 5.2. PERIODIC ORBIT ANALYSIS

The structure of the chaotic attractor can be characterized by a set of **unstable** periodic orbits (solutions of the differential equation), see [2]. The identification procedure will be based on a selection of these unstable periodic orbits. In order to extract periodic orbits from a Poincaré section of the (experimental) chaotic time series the phase space is partitioned in small boxes of linear size  $\varepsilon$  (1 % of the attractor size). A point that returns to either its own box or to a neighbouring box is called a recurrent point. The time it takes to return, gives the length of a candidate cycle. The list of candidate cycles is further reduced by requiring that a box contains at least a few points that  $\varepsilon$ -return as a  $p$  cycle. These points are used to determine a local linear approximation  $A^p$  of the dynamical system. A minimum of 32 neighbouring points  $y_t$ , taken from the neighbourhood of  $x_t^p$ , is included in the fit. The estimated stable and unstable eigenvalues of the periodic orbits are the eigenvalues of  $A^p$ . Fig. 5 shows the periodic points belonging to the cycles with period times up to length 5 that were found from an experimental time series of 42,754 points, see [2]. Note that a huge

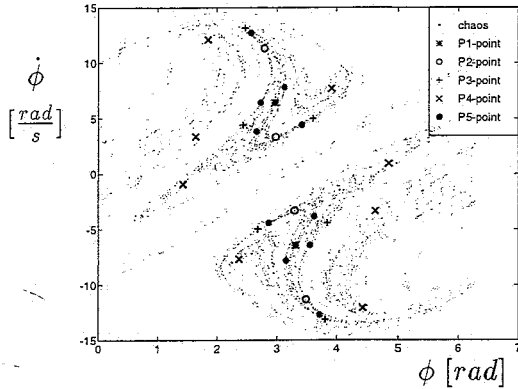


Figure 5. Poincaré section of the chaotic attractor and some low order, unstable periodic points

reduction of data has been obtained by extracting a few periodic points and their eigenvalues from a long chaotic time series. These unstable periodic points are now used to estimate parameters in the differential equation (10). It should be remarked that starting solutions for the periodic solver have to be chosen carefully otherwise convergence to other periodic solutions may result. Until now only the position in phase space ( $\phi$  and  $\dot{\phi}$  values) is used in the object function. In the future also the difference between estimated- and computed eigenvalues will be added to the object function.

### 5.3. RESULTS

The basis for the identification is equation (10) with  $\omega$  supposed to be known. From this equation it is clear that the parameters  $m, l, k_1, k_2$  and  $k_3$  can not be estimated simultaneously, because these parameters do not represent independent terms in the differential equation. The identification will therefore be split up in two parts namely (a) the estimation of  $m$  and  $l$  with fixed values for  $k_i, i = 1, 3$  and (b) estimation of  $k_3$  with known  $m, l$  and  $k_i, i = 1, 2$ . We only estimated friction parameter  $k_3$  because this is the largest term in the differential equation and variation of  $k_1$  and  $k_2$  showed to have only a small influence on the calculated unstable periodic solutions. As a reference we use a priori data for the friction parameters ( $k_{1exp}, k_{2exp}$ , and  $k_{3exp}$ ) as determined by [2] and values for  $m_{exp}$  and  $l_{exp}$  simply calculated from geometrical data. For the estimation, unstable periodic orbits up to period 5 were used. The results are presented in Table 1. From this

TABLE 1. Estimates of  $m, l$  and  $k_3$  with fixed  $k_1$  and  $k_2$

Initial state	$\frac{\dot{m}_0 - m_{exp}}{m_{exp}} = 51\%$	$\frac{l_0 - l_{exp}}{l_{exp}} = 18.9\%$	$\frac{k_{30} - k_{3exp}}{k_{3exp}} = 100\%$
Final state	$\frac{\dot{m} - m_{exp}}{m_{exp}} = 9.6\%$	$\frac{l - l_{exp}}{l_{exp}} = 0.3\%$	$\frac{k_3 - k_{3exp}}{k_{3exp}} = 11.6\%$

table, it can be concluded that  $l$  can be estimated very accurately, using the experimental data. However, the estimation of  $m$  and  $k_3$  are less accurate. This can be caused by the fact that the experimental time series was relatively short and contaminated by noise and the (experimental) periodic points unfortunately had to be picked by hand from Fig. 5.

The accuracy of the estimate  $l$  is very good and the estimates  $m$  and  $k_3$  are very acceptable given the level of measurement noise on the data.

## 6. Conclusions

In general it can be concluded that a nonlinear parameter identification method based on a set of stable and/or unstable periodic solutions com-



bined with the Bayesian estimation procedure has proven to be a powerful tool for the identification of parameters in a broad range of nonlinear dynamic systems. For the landing gear holds:

- A procedure based on periodic orbits is computationally far more efficient than a procedure based on transient signals.
- The thermo-dynamical part of the model should be improved.
- The identification procedure can be used as a quality-control instrument for landing gear production.

For the pendulum problem the following remarks can be made:

- By using periodic points instead of a chaotic trajectory, huge data reduction has been accomplished without losing essential information.
- A more comprehensive method in finding suitable starting solutions for the periodic solver is desirable.
- The introduction of the eigenvalues of the unstable periodic orbits in the object function should be investigated.
- The difficult numerical computation (due to positive Lyapunov exponents) of chaotic trajectories for very long times is not needed.

## Acknowledgements

The landing gear research was partially supported by DAF Special Products, Eindhoven, The Netherlands, and the authors thank Willem van de Water for helpful discussions and putting the pendulum experimental data at their disposal.

## References

1. Fey, R.H.B., Van de Vorst, E.L.B., Van Campen, D.H., De Kraker, A., Meijer, G.J., Assinck, F.H., 1994. *Chaos and Bifurcations in a multi-dof beam system with nonlinear support*, In: Nonlinearity and Chaos in Engineering Dynamics, J.M.T. Thompson and S.R. Bishop, editors, John Wiley & Sons, 125–139
2. Van de Water, W., Hoppenbrouwers, M., & Christiansen, F., 1991, *Unstable periodic orbits in the parametrically excited pendulum*, Physical Review A, **44**, 6388–6398.
3. Van de Wouw, N., Verbeek, G., Van Campen, D.H., 1995, *Nonlinear Parametric Identification Using Chaotic Data*, Jnl. of Vibration and Control, **1**, 291–305
4. Verbeek, G. 1993, *Nonlinear parametric identification using periodic equilibrium states, with application to a landing gear damper*, Ph.D. thesis, Eindhoven University of Technology.
5. Verbeek, G., de Kraker, A., & van Campen, D.H., 1995, *Nonlinear parametric identification using periodic equilibrium states, with application to a landing gear damper*, Nonlinear Dynamics, **7**, 499–515.